**Pavlo HERASYMENKO**

Institute of Electrodynamics of the National Academy of Sciences of Ukraine
ORCID: 0000-0001-6244-1133

# Augmented PDM for series-resonant inverters

*Abstract. The main disadvantage of a pulse-density-modulated (PDM) voltage-source series-resonant inverter (SRI) is that the amplitude of the SRI output current fluctuates. To reduce the fluctuation, this paper presents an augmented PDM control method for the SRI. The proposed augmented PDM reduces the fluctuation in the amplitude of the SRI output current and requires fewer PDM sequences compared to the irregular PDM, and also provides a more uniform pulse density difference between PDM sequences compared to the inconstant PDM.*

*Streszczenie. Główną wadą falownika z rezonansem szeregowym (SRI) z modulacją gęstości impulsu (PDM) jest to, że amplituda prądu wyjściowego SRI ulega wahaniom. Aby zredukować fluktuację, w niniejszym artykule przedstawiono metodę rozszerzonej kontroli PDM dla SRI. Proponowany rozszerzony PDM zmniejsza fluktuację amplitudy prądu wyjściowego SRI i wymaga mniejszej liczby sekwencji PDM w porównaniu z nieregularnym PDM, a także zapewnia bardziej jednolitą różnicę gęstości impulsów między sekwencjami PDM w porównaniu z niestałym PDM. (**Rozszerzony PDM dla falowników z rezonansem szeregowym**)*

**Keywords:** control method, fluctuation, induction heating, pulse-density modulation, series-resonant inverter.
**Słowa kluczowe:** falownik, rezonans szeregowy, PDM.

### Introduction

Recently, the pulse density modulation (PDM) control method has often been applied to regulate the output current, voltage, or power in series-resonant inverters (SRIs) for various technologies [1-6], among which is induction heating [7,8]. The PDM control method ensures the operation of the SRI transistors with zero-voltage switching (ZVS) and quasi-zero current switching (quasi-ZCS). The main disadvantage of this method is a current amplitude fluctuation.

Basically, in the pulse-density modulated SRI (PDM-SRI), current regulation is achieved by varying durations of an injection interval, as well as a free-wheeling interval, which are formed by the modes of operation of the full-bridge topology. In the traditional/conventional PDM control method, these durations are an integer multiple of the SRI output voltage period (when the SRI is operating at a pulse density of 1) [6-8]. In the case of the regular PDM, there are one injection interval and one free-wheeling interval within the duration of a PDM sequence, as a consequence, amplitude fluctuations of the SRI output current are significant. To reduce the fluctuations, it is expedient that the injection interval is being distributed between the free-wheeling interval [9-11]. This type of PDM is called irregular or non-regular PDM and is generally the most commonly used.

Various enhanced PDM controls have been proposed [12-14]. The general idea of which is that the duration of the injection interval and the free-wheeling interval, or only the injection interval, is an integer multiple of the half-period of the SRI output voltage. But in these cases, the SRI output voltage contains a dc component [12,13] (which is not very suitable if a matching transformer is required), or the fluctuation reduction is not significant [14]. In the case of using the odd (3rd or 5th) harmonic operation method [15,16], which can be considered as a variant of the PDM control method, the frequency of the SRI output voltage is three, five, or more times less than the PDM-SRI with the pulse density of 1, as a result, the size of the matching transformer will be significant. In [17-19], the authors have combined the phase-shift control method and the PDM control method. But in the case where the phase-shift control acts between PDM patterns to provide smoother power regulation [17,18], the fluctuation is not less compared to the PDM control method, and the switching loss is much larger. And in the case of the combined control method in [19], the switching losses of the SRI transistors in

the range from 0 to 0.5 increase, and the amplitude fluctuations in the range from 0.5 to 1 do not decrease.
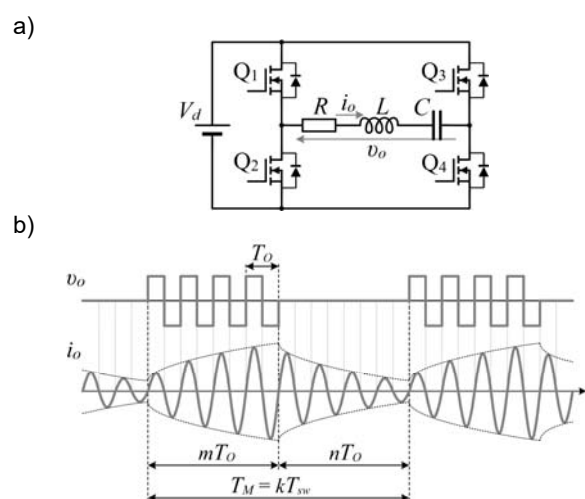
a)


b)


Fig.1. Schematic diagram of full-bridge PDM-SRI with output current $i_O$ and output voltage $v_O$ waveforms

Another approach to reducing the fluctuations is connected with the converter topologies (modular topology and extended topology) [20-23], which require more transistors, and the converter design is more complex; it is not particularly suitable for low to medium power equipment.

This paper discusses the amplitude fluctuation of the PDM-SRI output current and proposes an augmented PDM control method. The proposed control method allows to reduce the amplitude fluctuation of the SRI output current compared to the irregular PDM and requires fewer PDM sequences, and also provides a more uniform pulse density difference between them compared to the inconstant PDM. The proposed method is suitable for all mentioned above topologies.

### System configuration and operation

A schematic diagram of a full-bridge PDM-SRI with the output current $i_O$ and output voltage $v_O$ waveforms are shown in Fig. 1. The secondary components of the matching transformer are reflected to the primary side and represented as equivalent parameters; resistance $R$, inductance $L$, and capacitance $C$ are components of the series-resonant circuit connected to the SRI output.
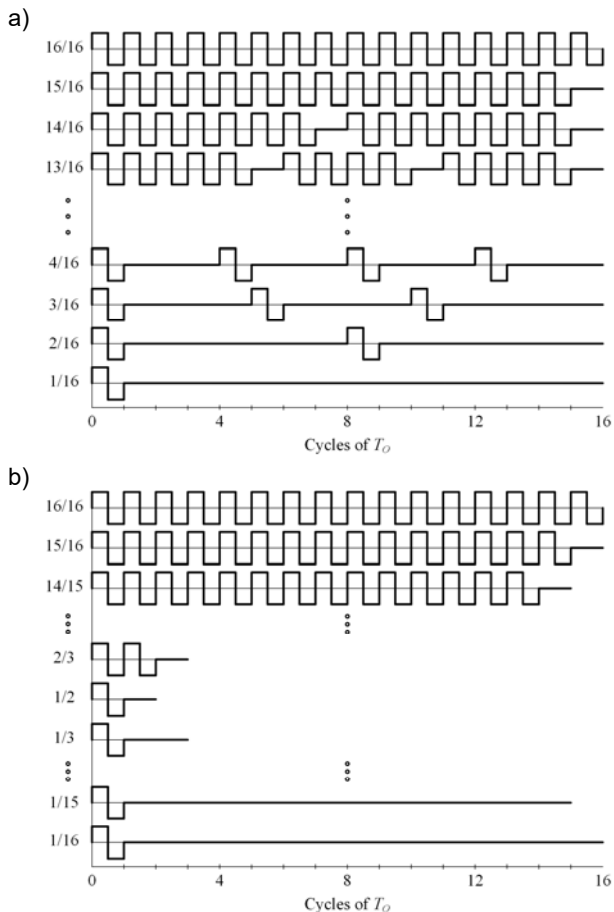
Fig.2. PDM patterns: (a) irregular PDM; (b) inconstant PDM

To provide the injection interval, the full-bridge PDM-SRI operates as a conventional full-bridge SRI and produces a square-wave ac-voltage state ($v_O = \pm V_d$) during $m$ cycles of the period $T_O$ of $v_O$; to provide the free-wheeling interval, the SRI acts as a zero-voltage source during $n$ cycles of $T_O$ (Fig. 1,b).

The duration $T_M$ of a PDM sequence can be expressed as follows:

$$(1) \qquad T_M = kT_O = (m+n)T_O$$

where $k$ is the number of cycles of $T_O$ during $T_M$; $m$ is the number of cycles of $T_O$ during the injection interval, and $n$ is the number of cycles of $T_O$ during the free-wheeling interval.

The frequency of PDM sequences is given by

$$(2) \qquad f_{PDM} = 1/T_M .$$

The pulse density $D$ of PDM patterns can be expressed as follows:

$$(3) \qquad D = m/k .$$

**Modulation principles**

Fig. 2,a shows the PDM patterns of the irregular PDM for a constant $k$-value of 16. Compared to the regular PDM (Fig. 1,b), in the irregular PDM, the injection and free-wheeling cycles are distributed among $T_M$ in such a way as to reduce the amplitude fluctuation of $i_O$. Both the regular PDM and the irregular PDM operate with a constant $k$-value. It is possible to vary the $k$-value in the mentioned PDMs, but this will lead to a significant increase in different variants of PDM patterns, often with the same $D$-value, which is unnecessary.

Another approach in forming PDM patterns is to change the $D$-value by changing the $k$-value (Fig. 2,b). This approach can be called inconstant PDM. In this case, in the range of $D$ from 1 to 0.5, there is no more than one free-wheeling interval (equal to $T_O$) during $T_M$, and in the range of $D$ from 0.5 to 0, there is no more than one injection interval (equal to $T_O$) during $T_M$. Compared to the irregular PDM, for the same maximal $k$-value, the inconstant PDM has more PDM patterns (e.g., at $k_{max} = 16$, the irregular PDM has 17 patterns and the inconstant PDM has 31 patterns). On the other hand, the irregular PDM has a constant difference of $D$ between two nearby PDM sequences, whereas the inconstant PDM doesn't.

With a high $k$-value, a more accurate power transfer resolution can be obtained [9]; however, this can lead to problems with acoustic noise (if $f_{PDM}$ is up to 20 kHz) [24] and slow response to changes in current or power feedback.

**Current amplitude fluctuations**

The fluctuation can be estimated from the peak-to-peak value of the envelope of $i_O$ [12] or the absolute peak-to-peak value of the amplitude of $i_O$ [23]. In the case of the irregular PDM, the absolute peak-to-peak value of the amplitude of $i_O$ is easier to determine by numerical computation or from simulation results, while the determination of the envelope of $i_O$ is difficult owing to changes in PDM patterns.

To provide current or power regulation, a control system monitors the change in the feedback signal between $i_O$ and the level of the current task signal and, based on the feedback level, selects the appropriate PDM sequence. Since the control system is limited in the choice of PDM sequences, if there is no appropriate PDM sequence to achieve the required value of $D$, the control system will change two nearby PDM sequences whose values of $D$ are closest to the desired one (Fig. 3). In such a way, the fluctuation level has to be determined as the difference between maximal and minimal amplitudes of $i_O$ of the two involved PDM sequences; the normalized value of the peak-to-peak current amplitude is given by

$$(4) \qquad \Delta I_m^* = \left[ I_{max}(D_{i+1}) - I_{min}(D_i) \right]/I_m$$

where $D_{i+1}$ and $D_i$ are the pulse densities of the two involved PDM sequences, $I_m$ is the maximum current amplitude in the case of $D = 1$.
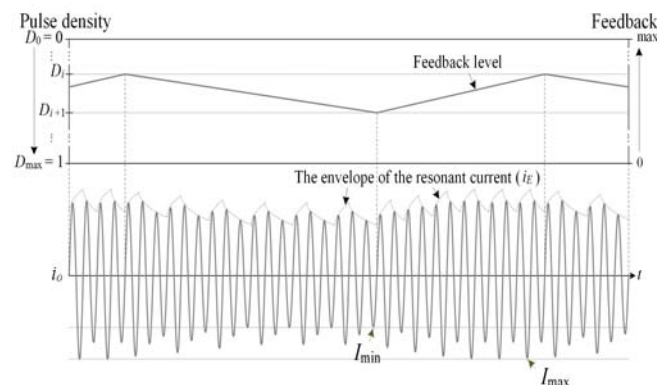


Fig.3. Output current waveform in case of cycling between two nearby PDM sequences

The output current $i_O(t)$ and the voltage $v_C(t)$ across the resonant capacitor $C$ in the time domain are given by [19]

$$(5) \qquad i_O(t) = I_{0x}\cos(\omega_d t)e^{-\frac{R}{2L}t} +$$

$$\frac{-\dfrac{RI_{0x}}{2} + \mathrm{sgn}(V_d)V_d - V_{0x}}{L\omega_d}\sin(\omega_d t)e^{-\frac{R}{2L}t},$$

$$(6) \qquad \upsilon_C(t) = \mathrm{sgn}(V_d)V_d + \left(V_{0x} - \mathrm{sgn}(V_d)V_d\right)\cos(\omega_d t)e^{-\frac{R}{2L}t} +$$

$$\left(\frac{I_{0x}}{\omega_d C} + \frac{R}{2L\omega_d}\left(V_{0x} - \mathrm{sgn}(V_d)V_d\right)\right)\sin(\omega_d t)e^{-\frac{R}{2L}t}$$

where: $\omega_d$ is the damped frequency, and $\mathrm{sgn}(V_d)$ is the sign function of $V_d$ are given by

$$(7) \qquad \omega_d = \sqrt{\frac{1}{LC} - \frac{R^2}{4L^2}},$$

$$(8) \qquad \mathrm{sgn}(V_d) = \begin{cases} 1; \\ 0; \\ -1. \end{cases}$$
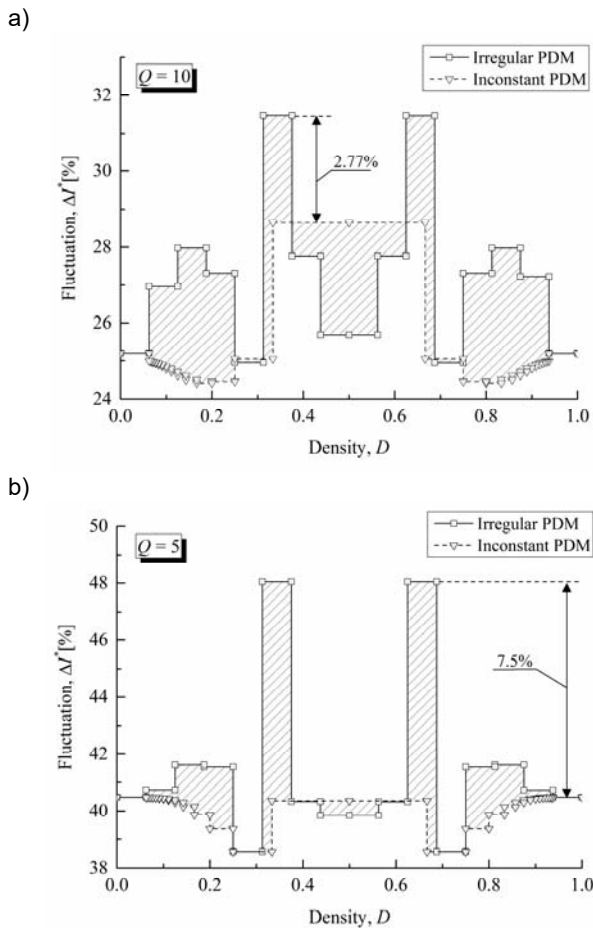
a)



b)



Fig.4. Fluctuation characteristics under different PDMs: (a) $Q = 10$; (b) $Q = 5$

Due to the fact that the operation of the PDM-SRI transistors occurs with quasi-ZCS, it is possible to simplify $I_0 = 0$. This simplification in (5) and (6) yields

$$(9) \qquad i_O(t) = \frac{\mathrm{sgn}(V_d)V_d - V_{0x}}{L\omega_d}\sin(\omega_d t)e^{-\frac{R}{2L}t},$$

$$(10) \quad \upsilon_C(t) = \mathrm{sgn}(V_d)V_d + \left(V_{0x} - \mathrm{sgn}(V_d)V_d\right)\cos(\omega_d t)e^{-\frac{R}{2L}t} +$$

$$\frac{R}{2L\omega_d}\left(V_{0x} - \mathrm{sgn}(V_d)V_d\right)\sin(\omega_d t)e^{-\frac{R}{2L}t}.$$

Fig. 4 shows relationships between the amplitude fluctuations of both the irregular PDM and the inconstant PDM as functions of $D$, which were obtained for the steady-state by (9) and (10) with the numerical computation at $k_{max}$ = 16. It can be seen in Fig. 4,a that when a quality factor $Q$ of the resonant circuit is equal to 10, there is no significant difference between the fluctuations of the mentioned PDMs. The maximal fluctuation value of the irregular PDM exceed the maximal fluctuation of the inconstant PDM by no more than 10%, which is only 2.77% of the amplitude of $i_O$ at $D$ = 1. On the other hand, at $Q$ = 5, the difference is more significant (Fig. 4,b); the maximal fluctuations of the irregular PDM exceed the maximal fluctuations of the inconstant PDM by almost 20%, which is 7.5% of the amplitude of $i_O$ at $D$ = 1. It can also be seen that the inconstant PDM has an excess amount of the PDM sequences, many of which can be neglected. On the other hand, there is a significant difference in values of $D$ between some PDM patterns.

At both $Q$ = 5 and $Q$ = 10, the irregular PDM has two spikes in the fluctuation graph. This is because some of the sequences of the irregular PDM contain unequal series of PDM sub-patterns (Fig. 5), as a consequence, more than two sub-patterns are used for two nearby PDM sequences. In contrast, all sequences of the inconstant PDM are unique patterns provided by a corresponding combination of the PDM parameters $(k;m;n)$; as a consequence, there are no significant spikes on the fluctuation graph.

**Proposed augmented PDM**
To reduce the fluctuations, it is expedient to use PDM sequences with unique patterns, as in the case of the inconstant PDM, and to exclude some PDM sequences in order to decrease the amount of the PDM sequences and provide a more uniform step in values of $D$ of nearby sequences, as in the case of the irregular PDM. At the same time, it is sensible to combine nearby PDM sequences in order to decrease the difference between their values of $D$; in this case, no more than two sub-patterns will be used for two nearby PDM sequences. Besides, even under a set $k_{max}$-value, to increase response to changes in current or power feedback it is possible to decrease $k$-values for the sequences with $D$ = 1 and $D$ = 0. Based on the above, Fig. 6 shows the patterns of the proposed augmented PDM. Along with the irregular PDM and the inconstant PDM, the augmented PDM control method also is suitable for the full-bridge, extended, and modular topologies.
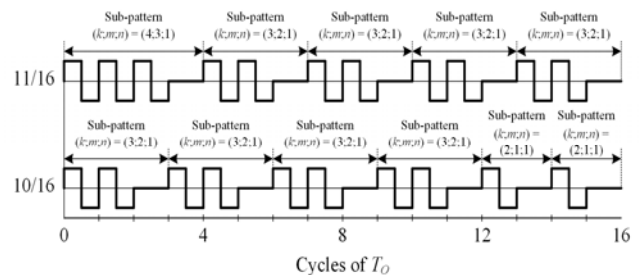


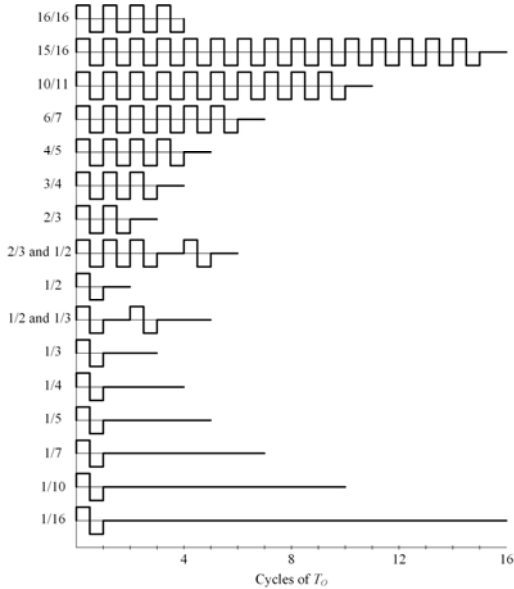Fig.5. Sub-patterns within PDM sequences in case of the irregular PDM

Fig.6. Patterns of the augmented PDM at $k_{max}$ = 16

Fig. 7 shows relationships between fluctuations of the irregular, inconstant, and augmented PDMs at $k_{max}$ = 16. It can be seen that the augmented PDM provides fewer fluctuations compared to the irregular PDM both at $Q$ = 5 and $Q$ = 10, as well as the inconstant PDM at $Q$ = 10. In addition, the fluctuating reduction is achieved with the same number of PDM sequences as in the irregular PDM, which is significantly less compared to the inconstant PDM; this may be important for implementation.
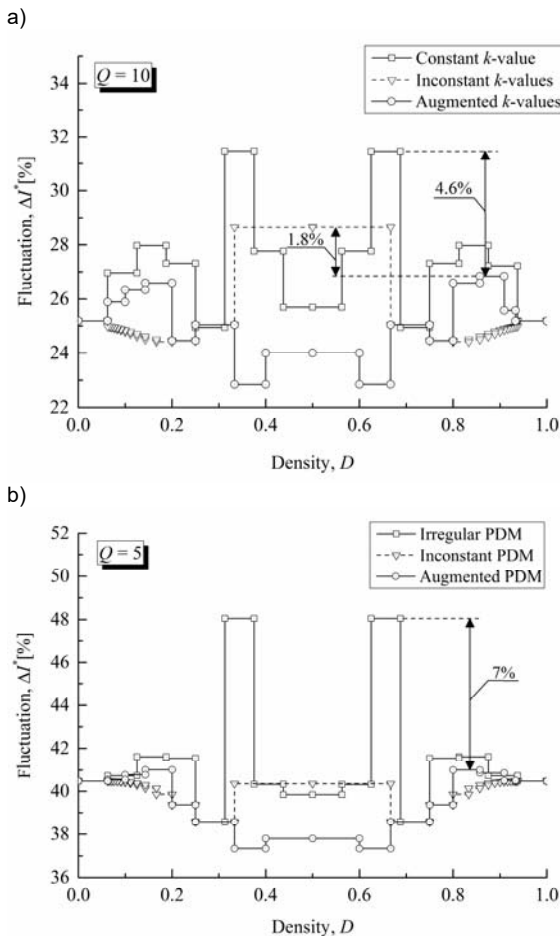
a)



b)



Fig.7. Fluctuation characteristics of the augmented PDM versus the irregular and inconstant PDMs

The fluctuations graphs in Fig. 7 show that using the augmented PDM makes it is possible to decrease fluctuations up to 4.6% of the amplitude of $i_O$ at $Q$ = 10 and, more importantly, up to 7% of the amplitude of $i_O$ at $Q$ = 5, without any changes in the topology of the SRI, or significant modification in the control algorithm.

In order to verify the correctness of the presented results obtained by the numerical computation, a simulation verification was carried out for some of the augmented DPM sequences. The simulation showed that the discrepancy between the result of numerical computation and simulation is no more than 0.2%.

**Conclusion**

This paper analyzes of PDM sequences for various types of PDM control and proposes an augmented PDM control method that:

1) reduces fluctuations in the amplitude of the SRI output current by 7% of the amplitude of the SRI output current at a quality factor of 5 and 4.6% at a quality factor of 10 compared to the irregular PDM;

2) requires fewer PDM sequences and provides a more uniform difference between the pulse density of two nearby PDM sequences compared to the inconstant PDM.

***Authors***: *Ph.D. Pavlo Herasymenko, Senior Researcher of Department of Transistor Converters, Institute of Electrodynamics of the National Academy of Sciences of Ukraine, 56 Peremohy Avenue, office 457, 03057, Kyiv, Ukraine, E-mail: herasymenko@ieee.org.*

REFERENCES
[1] Fan M., Shi L., Yin Z., Jiang L., Zhang F., Improved Pulse Density Modulation for Semi-bridgeless Active Rectifier in Inductive Power Transfer System, *IEEE Trans. on Power Electron.*, 34 (2019), No. 6, 5893-5902
[2] Li H., Fang J., Chen S., Wang K., Tang Y., Pulse Density Modulation for Maximum Efficiency Point Tracking of Wireless Power Transfer Systems, *IEEE Trans. on Power Electron.*, 33 (2018), No. 6, 5492-5501
[3] Setiadi H., Fujita H., Light-Load Switching-Loss Elimination Utilizing Pulse Density Modulation for Switched-Capacitor-Based Resonant Converters, *Proc. IEEE ECCE*, (2019), 4734-4740
[4] Sheng X., Shi L., An Improved Pulse Density Modulation Strategy Based on Harmonics for ICPT System, *IEEE Trans. on Power Electron.*, 35 (2020), No. 7, 6810-6819
[5] Wu T., Hung J., A PDM controlled series resonant multi-level converter applied for X-ray generators, *Proc. IEEE Power Electron. Specialists Conf.*, 2 (1999), 1177-1182
[6] Fujita H., Akagi H., Control and performance of a pulse-density-modulated series-resonant inverter for corona discharge processes, *IEEE Trans. on Ind. Appl*, 35 (1999), No. 3, 621-627
[7] Fujita H., Akagi H., Pulse-density-modulated power control of a 4 kW, 450 kHz voltage-source inverter for induction melting applications, *IEEE Trans. on Ind. Appl.*, 32 (1996), No. 2, 279-286
[8] Esteve V. et al., Improving the Efficiency of IGBT Series-Resonant Inverters Using Pulse Density Modulation, *IEEE Trans. on Ind. Electron.*, 58 (2011), No. 3, 979-987
[9] Sandali A., Cheriti A., Sicard P., Comparison of the various PDM control modes, *Proc. IEEE ICIT*, 2 (2004), 574-5792
[10] Calleja H., Pacheco J., Power distribution in pulse-density modulated waveforms, *Proc. IEEE 31st Annual Power Electron. Specialists Conf.*, 3 (2000), 1457-1462
[11] Karafil A., Ozbay H., Oncu S., Comparison of regular and irregular 32 pulse density modulation patterns for induction heating, *IET Power Electron.*, 14 (2020), No. 1, 1-12
[12] Esteve V. et al., Enhanced Pulse-Density-Modulated Power Control for High-Frequency Induction Heating Inverters, *IEEE Trans. on Ind. Electron.*, 62 (2015), No. 11, 6905-6914

[13] Sheng X., Shi L., Fan M., An Improved Pulse Density Modulation of High-Frequency Inverter in ICPT System, *IEEE Trans. on Ind. Electron.*, 68 (2021), No. 9, 8017-8027

[14] Herasymenko P.Y., A transistor resonant voltage inverter with pulse density modulation for induction heating equipment, *Technical Electrodynamics*, (2015), No. 6, 24-28

[15] Uesugi Y., Imai T., Kawada K., Takamura S., Fundamental and third harmonic operation of SIT inverter and its application to RF thermal plasma generation, *Proc. Power Conversion Conf.*, 3 (2002), 1473-1478

[16] Swadowski M., Zygon K., Jąderko A., High-frequency converters with resonant circuits working with multiple converter frequency on an example of use in induction heaters, *Przeglad Elektrotechniczny*, 94 (2018), No. 5, 143-146 (in Polish)

[17] Shen J., Ma H., Yan W., Hui J., L. Wu, PDM and PSM Hybrid Power Control of a Series-Resonant Inverter for Induction Heating Applications, *Proc. IEEE ICIEA*, (2006), 1-6

[18] Namadmalan A., Universal Tuning System for Series-Resonant Induction Heating Applications, *IEEE Trans. on Ind. Electron.*, 64 (2017), No. 4, 2801-2808

[19] Herasymenko P., Combined PS-PDM control method for voltagesource series-resonant inverter, *Przeglad Elektrotechniczny*, 97 (2021), No. 5, 40-45

[20] Zied H.A., Mutschler P., Bachmann G., A Modular IGBT Converter System for High Frequency Induction Heating Applications, *PCIM Conference*, (2002)

[21] Sarnago H., Lucía Ó., Burdío J.M., Interleaved Resonant Boost Inverter Featuring SiC Module for High-Performance Induction Heating, *IEEE Trans. on Power Electron.*, 32 (2017), No. 2, 1018-1029

[22] Herasymenko P., Pavlovskyi V., Soft Start-up Strategy of Pulse-Density-Modulated Series-Resonant Converter for Induction Heating Application, *Int. Journal of Power Electron. and Drive Sys.*, 12 (2021), No. 1, 258-272

[23] Herasymenko P., Yurchenko O., An Extended Pulse-Density-Modulated Series-Resonant Inverter for Induction Heating Applications, *Proc. IEEE RTUCON*, (2020), 1-8

[24] Moo C., Huang C., Yang C., Acoustic-Resonance-Free High-Frequency Electronic Ballast for Metal Halide Lamps, IEEE Trans. on Ind. Electron., 55 (2008), No. 10, 3653-3660